

This work was supported by the Department of Chemistry at Purdue University and the Center for Materials Research (grant No. 91-0285) at Michigan State University. We thank Kurt Mislow (NSF grant CHE-8510067) for support of preliminary work.

### References

- ANDERSEN, P. & KLEWE, B. (1967). *Acta Chem. Scand.* **21**, 2599.  
 BALLESTER, M., RIERA, J., CASTANER, J., BADIA, C. & MONSÓ, J. M. (1971). *J. Am. Chem. Soc.* **93**, 2215.  
 BYE, E., SCHWEIZER, W. B. & DUNITZ, J. D. (1982). *J. Am. Chem. Soc.* **104**, 5893–5898.  
 Cambridge Structural Database (1989). Cambridge Crystallographic Data Centre, Cambridge, England.  
 CROMER, D. T. & WABER, J. T. (1974). *International Tables for X-ray Crystallography*, Vol. IV, Table 2.2B. Birmingham: Kynoch Press. (Present distributor Kluwer Academic Publishers, Dordrecht.)  
 FRENZ, B. A. (1978). *The Enraf-Nonius CAD-4 SDP – A Real-Time System for Concurrent X-ray Data Collection and Crystal Structure Solution. Computing in Crystallography*, edited by H. SCHENK, R. OLTJOF-HAZEKAMP, H. VAN KONIGVELD & G. C. BASSI, pp. 64–71. Delft Univ. Press.  
 GILBERT, K. & GAJEWSKI, J. J. (1989). *PCMODEL*. Serena Software, Bloomington, Indiana, USA.  
 HAYES, K. S., NAGAMO, M., BLOUNT, J. F. & MISLOW, K. (1980). *J. Am. Chem. Soc.* **102**, 2773–2776.  
 JACKSON, J. E. & JANG, S.-H. (1990). Unpublished results.  
 KAHR, B. (1988). Dissertation, Princeton Univ., USA.  
 KAHR, B. & JACKSON, J. E. (1985). Unpublished results.  
 MAIN, P., FISKE, S. J., HULL, S. E., LESSINGER, L., GERMAIN, G., DECLERCQ, J.-P. & WOOLFSON, M. M. (1982). *MULTAN82. A System of Computer Programs for the Automatic Solution of Crystal Structures from X-ray Diffraction Data*. Univs. of York, England, and Louvain, Belgium.  
 MARTIN, J. C. & SMITH, R. G. (1964). *J. Am. Chem. Soc.* **86**, 2252–2256.  
 MISLOW, K. M. (1976). *Acc. Chem. Res.* **9**, 26–33; and references therein.  
 OLMSTEAD, M. M. & POWER, P. E. (1986). *J. Am. Chem. Soc.* **108**, 4235–4236.  
 SABACKY, M. J., JOHNSON, C. S. JR, SMITH, R. G., GUTOWSKY, H. S. & MARTIN, J. C. (1967). *J. Am. Chem. Soc.* **89**, 2054–2058.  
 SHELDRIK, G. M. (1986). *SHELXS86*. Program for the solution of crystal structures. Univ. of Göttingen, Germany.  
 VECIANA, J., CARILLA, J., MIRAVITLLES, C. & MOLINS, E. (1987). *J. Chem. Soc. Chem. Commun.* p. 812.  
 WALKER, N. & STUART, D. (1983). *Acta Cryst.* **A39**, 158–166.  
 ZACHARIASEN, W. H. (1963). *Acta Cryst.* **16**, 1193.

*Acta Cryst.* (1992). **B48**, 329–336

## Neutron Diffraction and Calorimetric Studies of Methylammonium Iodide\*

BY O. YAMAMURO, T. MATSUO AND H. SUGA

*Department of Chemistry and Chemical Thermodynamics Laboratory, Faculty of Science, Osaka University, Toyonaka, Osaka 560, Japan*

AND W. I. F. DAVID, R. M. IBBERSON AND A. J. LEADBETTER†

*ISIS Science Division, Rutherford Appleton Laboratory, Chilton, Didcot, Oxfordshire OX11 0QX, England*

(Received 22 July 1991; accepted 7 January 1992)

### Abstract

A powerful combination of calorimetric and high-resolution neutron powder-diffraction techniques has been used to study the phase transitions in deuterated methylammonium iodide. The neutron powder-diffraction measurements have confirmed the four-fold disorder of the deuterium atoms about the  $C_3$  axis of the methylammonium ion in the tetragonal ( $P4/nmm$ )  $\alpha'$  phase. The structure of the metastable  $\delta$  phase was determined using a novel method of chemically constrained profile refinement. It was found to be orthorhombic ( $Pbma$ ,  $Z = 4$ ,  $a = 7.1743$ ,  $b = 7.0967$ ,  $c = 8.8323$  Å) in which the deuterium

atoms were completely ordered in an anti-parallel manner along the  $b$  axis. Heat capacities of the  $\alpha'$  and  $\delta$  phases of  $CD_3ND_3I$  were measured in the temperature range 13–303 K. A continuous  $\lambda$ -type anomaly was found at the  $\delta$ - $\alpha'$  phase transition which occurred at 164.0 K with an associated transition entropy of  $8.8 \text{ J K}^{-1} \text{ mol}^{-1}$ . The results are very similar to those of  $CH_3NH_3I$  measured previously, indicating that deuteration of the methylammonium ion does not affect the mechanism of the  $\delta$ - $\alpha'$  phase transition of  $CD_3ND_3I$ .

### 1. Introduction

$CH_3NH_3X$  ( $X = \text{Cl, Br, I}$ ) compounds have many polymorphs related to the various types of orientational disorder of the methylammonium ( $CH_3NH_3^+$ ) ion. In the high-temperature  $\epsilon$  phase (observed only

\* Contribution No. 19 from the Chemical Thermodynamics Laboratory.

† Present address: Daresbury Laboratory, Daresbury, Warrington WA4 4AD, England.

for I), the  $\text{CH}_3\text{NH}_3^+$  ion is disordered both with respect to the orientation around the C—N axis and to that of the C—N axis itself. In the moderate-temperature phases  $\alpha$  (for Cl and Br) and  $\alpha'$  (for Br and I), the orientation of the C—N axis is ordered but that around the C—N axis is still disordered. The remaining disorder is removed through two different phase transitions at low temperatures; *i.e.* to the stable  $\beta$  (for Cl and Br) or  $\beta'$  (for I) phases and to the metastable  $\delta'$  (for Cl) or  $\delta$  (for Br and I) phases. The  $\gamma$  phase appears only for the chloride between the  $\alpha$  and  $\beta$  phases. These rather complicated phase relations have been clarified by calorimetric (Aston & Ziemer, 1946; Yamamuro, Oguni, Matsuo & Suga, 1986a), DTA (Ishida, Ikeda & Nakamura, 1982a,b; Yamamuro, Oguni, Matsuo & Suga, 1986b) and IR (Cabana & Sandorfy, 1967; Théorêt & Sandorfy, 1967) studies. X-ray diffraction studies (Yamamuro, Oguni, Matsuo & Suga, 1986b) showed that the  $\epsilon$  phase has a CsCl-type cubic structure, and the  $\alpha$  and  $\alpha'$  phases have tetragonal structures belonging to the same space group of  $P4/nmm$ , where the C—N axis was uniquely oriented along the fourfold crystallographic axis (Hendricks, 1928; Hughes & Lipscomb, 1946; Stammler, 1967; Gabe, 1961). In these phases, however, the positions of H atoms of the  $\text{CH}_3\text{NH}_3^+$  ion have yet to be determined. Although no structural studies of the low-temperature  $\beta$ ,  $\beta'$ ,  $\delta$  and  $\delta'$  phases have been done, the  $\beta'$  and  $\delta'$  phases are expected to be the same as the  $\beta$  and  $\delta$  phases, respectively. The rotational motions of the  $\text{CH}_3\text{NH}_3^+$  ion have been most actively investigated by NMR (Yamamuro, Oguni, Matsuo & Suga, 1986b; Tsau & Gilson, 1970; Tegenfelt, Keowsim & Säterkvist, 1972; Albert & Ripmeester, 1973; Sundaram & Ramakrishna, 1982; Ishida, Ikeda & Nakamura, 1982a,b, 1986), NQR (Jugie & Smith, 1978), IR (Whalley, 1969), Raman (Castallucci, 1969) and inelastic neutron scattering (Ludman, Ratcliffe & Waddington, 1976) studies. They indicated that both the  $\text{CH}_3$  and  $\text{NH}_3^+$  groups were spinning rapidly around the C—N axis in the  $\epsilon$ ,  $\alpha$  and  $\alpha'$  phases, while the rotations became slow in the  $\gamma$ ,  $\beta$ ,  $\beta'$ ,  $\delta$  and  $\delta'$  phases (especially in the  $\beta$  and  $\beta'$  phases).

Methylammonium iodide,  $\text{CH}_3\text{NH}_3\text{I}$ , is the most interesting compound of those noted above because it is the only compound of this series in which both the stable  $\beta'$  and metastable  $\delta$  phases can be studied down to low temperature. The phase relationships of  $\text{CH}_3\text{NH}_3\text{I}$  may be represented schematically as shown in Fig. 1.

The supercooled metastable phases of  $\text{CH}_3\text{NH}_3\text{Cl}$  ( $\delta'$ ) and  $\text{CH}_3\text{NH}_3\text{Br}$  ( $\delta$ ) readily transform to the stable  $\beta$  phase on cooling. In addition the  $\epsilon$  phase can also only be observed in  $\text{CH}_3\text{NH}_3\text{I}$ . Recent calorimetric and dilatometric studies of  $\text{CH}_3\text{NH}_3\text{I}$

(Yamamuro, Oguni, Matsuo & Suga, 1986a) have shown that the phase transition from  $\beta'$  to  $\alpha'$  is first order with large supercooling and superheating effects, while that from  $\delta$  to  $\alpha'$  was of a higher-order nature. It also indicated that both the low-temperature phases were completely ordered at absolute zero from entropic considerations. Subsequent microscopic and dielectric studies (Yamamuro, Oguni, Matsuo & Suga, 1987) revealed that the metastable  $\delta$  phase adopted an orthorhombic or monoclinic structure in which the  $\text{CH}_3\text{NH}_3^+$  ions were ordered in an anti-ferroelectric manner.

In this study, we present high-resolution neutron powder-diffraction measurements of the  $\alpha'$  and  $\delta$  phases (the  $\beta'$  phase could not be obtained as described below) on the deuterated compound  $\text{CD}_3\text{ND}_3\text{I}$ . The purpose of the study was to determine the structures, including the positions of deuterium atoms associated with the  $\text{CD}_3\text{ND}_3^+$  ion, and to clarify the mechanism of the phase transition from a structural viewpoint. In order to examine the entropic aspect of the phase transition, the heat capacity of  $\text{CD}_3\text{ND}_3\text{I}$  was measured in the temperature range 13–303 K with an adiabatic calorimeter. Deuteration effects, such as shifts in the transition temperature, are most accurately studied by calorimetry which also revealed there to be no metastable–stable transition in the deuterated compound as is observed in the hydrogenous material.

## 2. Experimental

### 2.1. Sample preparation

The  $\text{CD}_3\text{ND}_3\text{I}$  sample used for the calorimetric and neutron powder-diffraction studies was prepared as follows.  $\text{CD}_3\text{NH}_2$  gas was produced by mixing  $\text{CD}_3\text{NH}_2\text{Cl}$  (>98 atom% D; Aldrich Chemical Company) and a saturated aqueous solution of NaOH. The  $\text{CD}_3\text{NH}_2$  gas was dissolved in HI – 50% aqueous solution (Wako Pure Chemical Industries Ltd), in which the amount of HI was slightly in excess compared with  $\text{CD}_3\text{NH}_2$ . Removal of the water and the excess HI by pumping gave  $\text{CD}_3\text{NH}_3\text{I}$ , which was recrystallized from ethanol and washed with chloroform. Deuteration of the  $\text{CD}_3\text{NH}_3\text{I}$  was performed by repeating the following procedure twice. The  $\text{CD}_3\text{NH}_3\text{I}$  was dissolved (40 times by

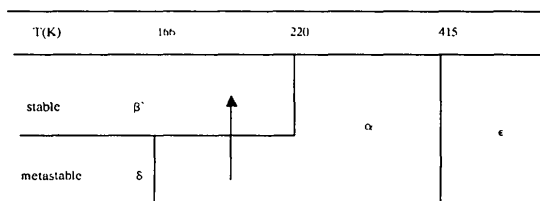


Fig. 1. Phase relationships of  $\text{CH}_3\text{NH}_3\text{I}$ .

volume) in degassed deuterated water (>99.75 atom% D; Aldrich Chemical Company) in a helium atmosphere, the subsequent water removal being carried out by vacuum distillation. All the procedures described above were carried out in the dark since  $\text{CD}_3\text{ND}_3\text{I}$ , especially in solution, is rapidly decomposed by light.

The following values show the result of the elemental analysis of  $\text{CD}_3\text{ND}_3\text{I}$  in mass%:

|       | C    | D    | N    | I     |
|-------|------|------|------|-------|
| Obs.  | 7.31 | 7.23 | 8.49 | 76.96 |
| Calc. | 7.28 | 7.33 | 8.49 | 76.90 |

All of the observed values agree with the calculated figures within an error of less than 0.1%. The deuteration level was calculated to be 99.73% by considering the ratio of deuterium to nitrogen.

## 2.2. Neutron diffraction measurements

Neutron powder-diffraction data of  $\text{CD}_3\text{ND}_3\text{I}$  were recorded at 4.2 K and room temperature using the high-resolution powder diffractometer (David, Akporiaye, Ibberson & Wilson, 1988), HRPD, at the spallation pulsed neutron source ISIS. Data were collected using 2 cm<sup>3</sup> of sample contained within a vacuum-tight vanadium can. Three time-of-flight regions 30–130, 100–210 and 180–280 ms were recorded. These regions correspond to a total *d*-spacing range from 0.6–5.6 Å. After the  $\alpha'$  phase data were collected at room temperature, subsequent rapid cooling to 4.2 K yielded the  $\delta$  phase. Attempts to obtain the  $\beta$  phase by annealing at temperatures just below the 160 K transition temperature were unsuccessful.

## 2.3. Heat-capacity measurement

The heat-capacity measurement was carried out over the temperature range 13–303 K using an adiabatic calorimeter described elsewhere (Tatsumi, Matsuo, Suga & Seki, 1975; Matsuo & Suga, 1985). The accuracy of  $C_p$  was better than 0.3% across the whole temperature range. The  $\text{CD}_3\text{ND}_3\text{I}$  sample was sealed in a calorimeter cell of volume 4.624 cm<sup>3</sup> with helium gas at atmospheric pressure to facilitate thermal contact between the cell and the sample. The mass of the sample used was 4.2582 g, corresponding to  $2.5806 \times 10^{-2}$  mol. The temperature increment for each measurement was 1–3 K in the normal region but was reduced to 0.1 K around the peak of the transition.

## 3. Results and discussion

### 3.1. The $\alpha'$ -phase structure (295 K)

At room temperature, methylammonium iodide has a tetragonal structure. The methylammonium

Table 1. Final structural and profile parameters for  $\alpha'$ - $\text{CD}_3\text{ND}_3\text{I}$  at 300 K

Tetragonal: space group  $P4/nmm$  (No. 129),  $a = 5.12729$  (1),  $b = 5.12729$  (1),  $c = 9.01794$  (2) Å. Deuterium site occupancies = 0.18750.  $R_f = 7.10\%$ ,  $R_{wp} = 5.17\%$ ,  $R_{exp} = 1.89\%$  and  $\chi^2 = 7.47$  for 4458 profile points and 17 basic variables.

|     | $x$           | $y$           | $z$          | $B_{iso}$ (Å <sup>2</sup> ) |
|-----|---------------|---------------|--------------|-----------------------------|
| N   | $\frac{1}{4}$ | $\frac{1}{4}$ | 0.20393 (21) | 4.09 (15)                   |
| C   | $\frac{1}{4}$ | $\frac{1}{4}$ | 0.36233 (30) | 7.91 (18)                   |
| I   | $\frac{1}{4}$ | $\frac{1}{4}$ | 0.81101 (45) | 3.88 (17)                   |
| D11 | $\frac{1}{4}$ | 0.06596 (–)   | 0.16490 (30) | 8.03 (17)                   |
| D12 | 0.11986 (–)   | 0.11986 (–)   | 0.16490 (30) | 8.03 (17)                   |
| D13 | 0.17957 (–)   | 0.07997 (–)   | 0.16490 (30) | 8.03 (17)                   |
| D21 | $\frac{1}{4}$ | 0.06596 (–)   | 0.40136 (21) | 8.03 (17)                   |
| D22 | 0.11986 (–)   | 0.11986 (–)   | 0.40136 (21) | 8.03 (17)                   |
| D23 | 0.17957 (–)   | 0.07997 (–)   | 0.40136 (21) | 8.03 (17)                   |

molecule is oriented along the tetragonal axis and is orientationally disordered about that axis since the free form axis of the molecule coincides with the fourfold crystallographic axis. Using the X-ray data of Hendricks (1928) as a starting point in the profile refinement, rapid convergence was obtained. The C—N bond is indeed aligned along the fourfold axis, and the disordered configuration of the methyl group was accurately fitted by a 12-site disordered model for the deuterium positions. However, because of the large thermal motion, it is impossible to distinguish between a 12-fold disorder and free rotation of the methyl groups about the tetragonal axis. For this reason it also proved difficult to refine the in-plane deuterium  $x$  and  $y$  coordinates and in the final refinement these values were fixed. The refined structural parameters are presented in Table 1. The large values for isotropic temperature factors, particularly up and down the  $c$  axis for the methyl group, may be an indication of a small degree of frozen-in disorder of the methylammonium orientation up and down the  $z$  axis.

### 3.2. The $\delta$ -phase structure

The powder-diffraction pattern obtained at 5 K clearly showed that a phase transition had occurred in agreement with the heat-capacity measurements discussed below, which indicated an order–disorder transition consistent with the ordering of the methylammonium ions about the  $c$  axis of the tetragonal structure. Although the continuous nature of the structural phase transition at 161 K between the  $\alpha'$  and  $\delta$  phases suggests that the low-temperature space group is a subgroup of the tetragonal space group  $P4_1/mmm$ , a preliminary inspection of the 5 K diffraction data revealed that a cell doubling had most probably occurred and that there was a significant distortion from the tetragonal phase indicative of orthorhombic or lower symmetry. The orthorhombic symmetry was indeed confirmed by traditional auto-indexing techniques. The positions of the highest

*d*-spacing reflections were manually measured for indexing purposes. Using the autoindexing program *TREOR* (Werner, 1976), the crystal lattice was indexed to an orthorhombic cell  $a = 7.1675$ ,  $b = 7.0919$ ,  $c = 8.8251$  Å (see supplementary material\*), indicating a  $\sqrt{2}$  by  $\sqrt{2}$  increase in cell size within the *ab* plane. This ease of lattice parameter determination from first principles is typical of time-of-flight powder diffraction experiments when the highest *d*-spacing information is available. This is because the zero-point error becomes progressively less important the larger the *d*-spacing in time-of-flight measurements, in contrast to the opposite effect for constant-wavelength measurements. Calculation of all possible *d*-spacings consistent with the orthorhombic cell obtained by autoindexing indicated that the orthorhombic structure possessed several systematic absences. These systematic absences were obtained using the following procedure. Instead of performing a traditional Rietveld profile refinement in which the unit cell, atomic coordinates and peak-shape parameters are varied, the present method involves the refinement of unit-cell constants and individual peak intensities. This technique was originally pioneered by Pawley (1981). The space group

assumed in the refinement was the orthorhombic group *Pmmm* since it possesses no systematic absences. The systematic absences and hence the correct space group are determined by examination of peak intensities which are less than three standard deviations in magnitude. The first 105 intensities extracted by this procedure have been presented for deposition. These intensities and the standard deviations were then automatically scanned for systematic presences. All reflections with intensities less than three standard deviations were rejected. The systematic presences indicated that for *Ok* reflections *k* must be even, and that for *hk*0 reflections *h* must be even. This is consistent with the extinction symbol *Pb*-*a* and with the space groups *Pbma* and *Pb*<sub>2</sub>*a* as presented in the supplementary material. Consideration of the eight possible ordering schemes of the molecule consistent with cell doubling, shown in Fig. 2, led to one space group conforming to *Pbma*. This is indicated in Fig. 3. Trial atomic coordinates were obtained from consideration of the high-temperature tetragonal structure. Basic packing considerations indicated that this initial trial structure may be a considerable distance from the final true solution. As traditional Rietveld profile refinement is invariably unstable if the initial structural guess is some way from the correct solution, the problem was restrained by constraining the methylammonium bond lengths to be fixed during the refinement. This has the effect of forcing the methylammonium ion to move as a rigid group and severely reduces the possible instabilities that may arise during profile refinement. This

\* Lists of autoindexing results, refined intensities, systematic presences, molar heat capacities and standard thermodynamic functions have been deposited with the British Library Document Supply Centre as Supplementary Publication No. SUP 54870 (7 pp.). Copies may be obtained through The Technical Editor, International Union of Crystallography, 5 Abbey Square, Chester CH1 2HU, England.

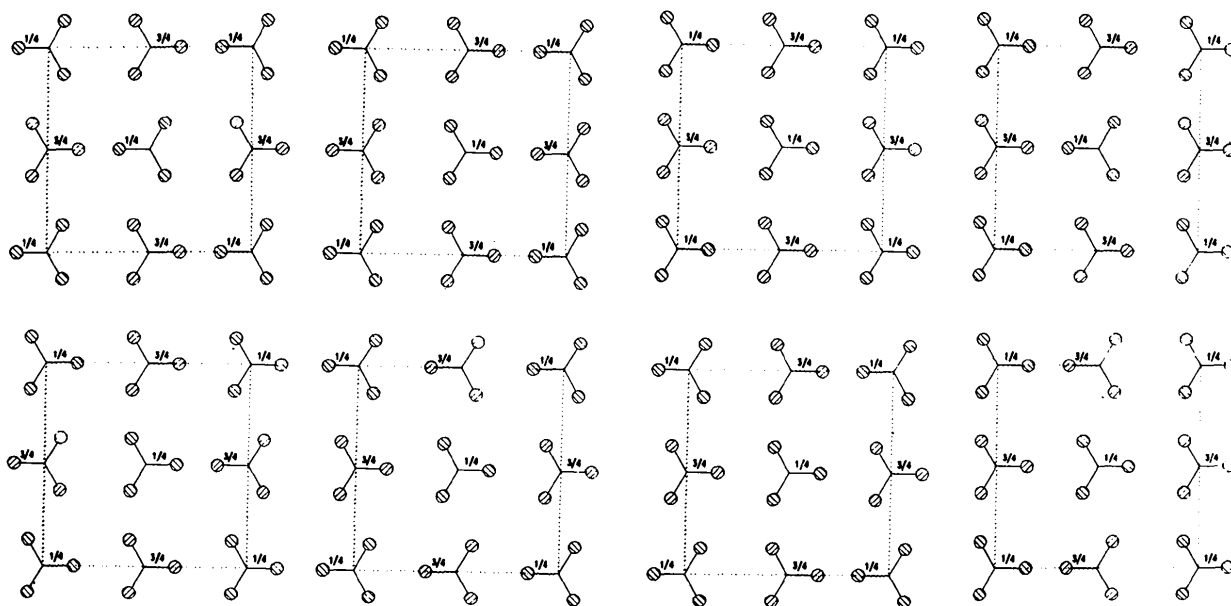


Fig. 2. Possible ordering schemes of the methyl groups for the  $\delta$ -phase structure derived from the  $\alpha$ -phase structure by a cell doubling. (The sections are drawn in the *ab* plane showing a fractional *z* coordinate for each group.)

technique, although similar in effect to the work of Pawley (1981), is different in that in the structure solution of  $\text{CF}_3\text{Cl}$ , Pawley & Hewat (1985) ensured that the molecule would move as a rigid body by reducing the number of parameters that were refined and used to describe the molecular coordinates. In the present work, the number of refined parameters is not reduced, rather the number of observations is increased by imposing strict chemical information to deal with very strongly constrained bond lengths. Nevertheless, the effect is equally dramatic. Both techniques yield an extremely robust refinement. Inspection of the calculated profiles, Fig. 4, at the end of each cycle graphically illustrate this. The intensity's  $R$  factor reduces from 112% to 30% in five cycles. This is consistent with an average atomic movement of greater than  $0.2 \text{ \AA}$ . The structure obtained using these strong slack constraints was subsequently refined using the traditional Rietveld method. The observed and calculated profiles and structural model are shown in Figs. 5 and 6 respectively. The final structural and profile parameters are given in Table 2.

### 3.3. Heat capacity

Heat capacities of the phases obtained by rapid cooling (*ca*  $5 \text{ K min}^{-1}$  around  $200 \text{ K}$ ) of the deuterated sample are plotted in Fig. 7 as open circles. The data of the metastable phases ( $\delta$  and  $\alpha'$ ) of  $\text{CH}_3\text{NH}_3\text{I}$  (Yamamuro, Oguni, Matsuo & Suga, 1986*a,b*) are plotted as closed circles. In  $\text{CH}_3\text{NH}_3\text{I}$ , the irreversible phase transition from the metastable  $\alpha'$  to the stable  $\beta'$  phase occurred just above the temperature of the  $\lambda$ -type transition from the  $\delta$  to  $\alpha'$  phase and made the  $C_p$  measurement of the  $\alpha'$  phase impossible in the temperature region  $175\text{--}215 \text{ K}$ . In the deuterated sample a similar  $\lambda$ -type transition was observed in the analogous temperature region. The

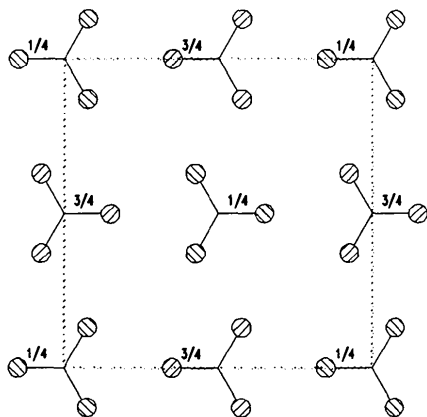


Fig. 3. Methyl-group ordering scheme consistent with the space group  $P6_3/m$ .

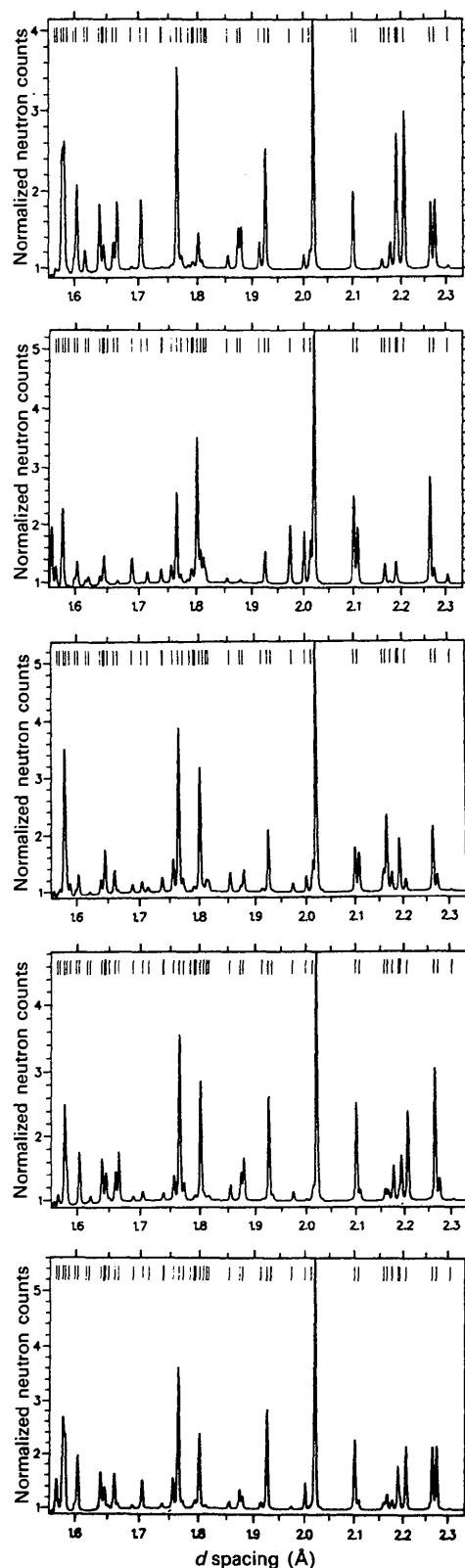


Fig. 4. Calculated profiles during the five cycles of constrained refinement of  $\delta$ -methylammonium iodide.

irreversible transition, however, did not occur. From the similarity of both heat-capacity curves, discussed below, the phases observed here should be  $\delta$  and  $\alpha'$ , corresponding to the phases of  $\text{CH}_3\text{NH}_3\text{I}$ . In fact, the neutron diffraction study shows that the high-temperature phase of  $\text{CD}_3\text{ND}_3\text{I}$  is the same as that of  $\text{CH}_3\text{NH}_3\text{I}$  ( $\alpha'$ ).

Factors that determine the metastability of the phases are not clear at present. However, because of the persistent metastability of the  $\alpha'$  phase of the deuterated sample, its heat capacity could be measured in the entire temperature region without being disrupted by the irreversible transformation to the  $\beta'$

phase. The result showed that the interpolation previously made in the  $C_p$  curve of  $\text{CH}_3\text{NH}_3\text{I}$  was justified. It is reasonable to assume the existence of the  $\beta$  phase for the deuterated compound although it has not been observed.

### 3.4. The $\delta$ to $\alpha'$ phase transition

The heat capacity was measured with a temperature increment of 0.1 K around the peak of the  $\lambda$ -type  $\delta$  to  $\alpha'$  transition. Even at the top of the peak, thermal equilibrium after heating was attained as rapidly as in the temperature range free from transition effects. This shows the transition to be of higher order as with  $\text{CH}_3\text{NH}_3\text{I}$ . The heat-capacity peak occurred at 164.0 K, which is lower than the peak temperature of  $\text{CH}_3\text{NH}_3\text{I}$  by 2.1 K, indicating a negative isotope effect.

In order to separate the transitional contribution from the normal heat capacity, the vibrational heat capacity (base line) was calculated using the following model heat-capacity function involving harmonic oscillators and hindered rotors with a small correction for the  $C_p - C_v$  difference:  $C_p(\text{base}) = C(\text{intra-ionic vibration}, 17, E) + C(\text{libration}, 2, E) + C(\text{lattice vibration}, 3, D) + C(\text{lattice vibration}, 3, E) + C(\text{internal rotation}, 1, M) + C(\text{overall rotation}, 1, M) + AC_p^2T$ , where  $E$  and  $D$  in the parentheses indicate the Einstein and Debye models respectively and  $M$  the heat capacity of a hindered rotor calculated by the use of the Mathieu energy levels. The two  $M$  terms represent the internal and external rotations of the methylammonium ion. Eigenvalues of the Mathieu equation involve the moment of inertia  $I$  of the rotors, symmetry number  $n$  and barrier height  $V_0$  as parameters, as described elsewhere (Yamamuro, Oguni, Matsuo & Suga, 1986a,b). The wavenumbers (in  $\text{cm}^{-1}$ ) of the 17 intra-ionic vibrations were taken from the IR data (Théorêt & Sandorfy, 1967): 2311 (1), 2129 (1), 1157 (1), 1082 (1), 891 (1), 2379 (2), 2181 (2), 1148 (2), 1038 (2), 1005 (2), 658 (2), where the numbers in parentheses denote the degeneracy. The librational wavenumber was determined to be  $101 \text{ cm}^{-1}$  by multiplication of the square root of  $I_H/I_D$  by the wavenumber of the corresponding mode in  $\text{CH}_3\text{NH}_3\text{I}$  [ $110 \text{ cm}^{-1}$ , after Ludman, Ratcliffe & Waddington (1976)]. The values  $I$ ,  $n$  and  $V_0$  for the internal and overall rotations of the  $\text{CD}_3\text{ND}_3^+$  ion were  $5.002 \times 10^{-47} \text{ kg m}^2$ , 3,  $9.9 \text{ kJ mol}^{-1}$  and  $20.08 \times 10^{-47} \text{ kg m}^2$ , 12,  $3.4 \text{ kJ mol}^{-1}$ , respectively. The values other than those for  $I$  were assumed to be the same as those of  $\text{CH}_3\text{NH}_3\text{I}$ .

The remaining three parameters, the Debye temperature  $\theta_D$  and Einstein temperature  $\theta_E$  for the lattice vibrations and a coefficient of the last term  $A$ , were determined using a least-squares fitting method.

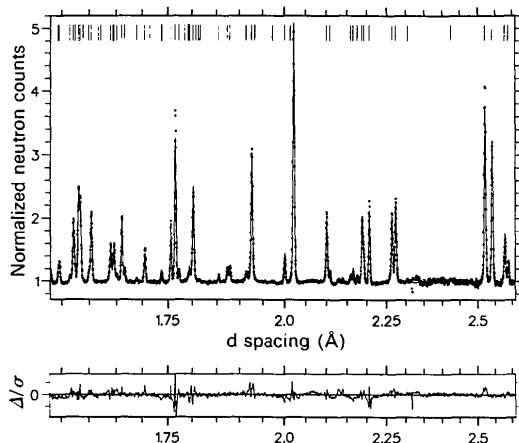


Fig. 5. Calculated and observed profiles for  $\delta$ -methylammonium iodide.

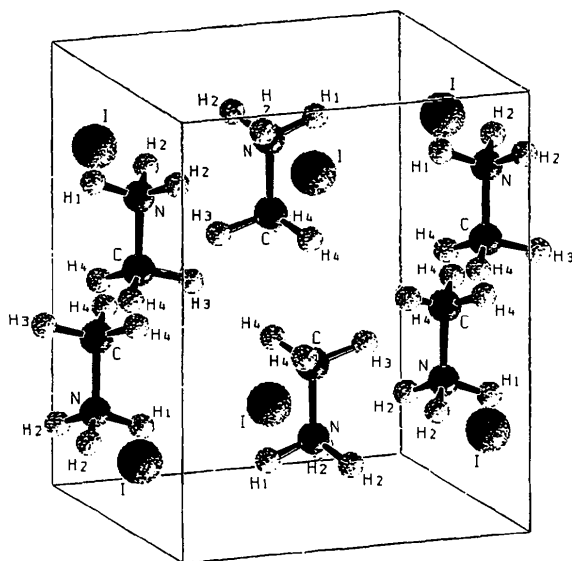


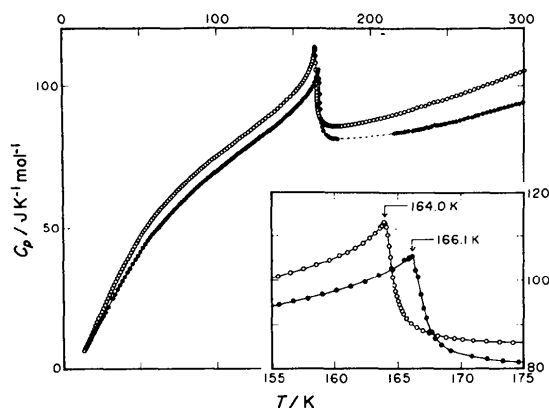
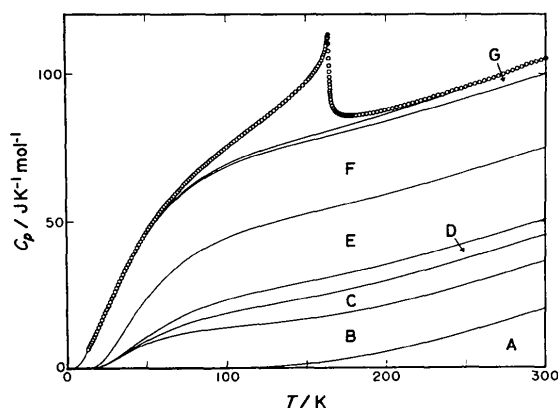
Fig. 6. SCHAKAL (Keller, 1988) illustration of  $\delta$ -methylammonium iodide.

Table 2. Final structural and profile parameters for  $\delta$  CD<sub>3</sub>ND<sub>3</sub>I at 5 K

Orthorhombic: space group *Pbma* (No. 57),  $a = 7.17143$  (2),  $b = 7.09673$  (2),  $c = 8.83232$  (2) Å.  $R_I = 3.93\%$ ,  $R_{wP} = 3.33\%$ ,  $R_{exp} = 1.22\%$  and  $\chi^2 = 7.43$  for 3510 profile points and 61 basic variables.

|    | $x$           | $y$            | $z$          | $B_{11}$ (Å <sup>2</sup> ) | $B_{22}$ (Å <sup>2</sup> ) | $B_{33}$ (Å <sup>2</sup> ) |
|----|---------------|----------------|--------------|----------------------------|----------------------------|----------------------------|
| N  | -0.03011 (43) | $-\frac{1}{4}$ | 0.20779 (40) | 0.23 (10)                  | 1.39 (12)                  | 1.75 (13)                  |
| C  | -0.03312 (65) | $-\frac{1}{4}$ | 0.37551 (43) | 1.95 (17)                  | 0.97 (17)                  | 1.48 (21)                  |
| I  | -0.02886 (52) | $-\frac{1}{4}$ | 0.81006 (50) | 0.52 (14)                  | 0.25 (13)                  | 0.25 (13)                  |
| D1 | -0.16182 (68) | $-\frac{1}{4}$ | 0.16664 (46) | 2.92 (21)                  | 2.67 (21)                  | 1.41 (23)                  |
| D2 | 0.03352 (39)  | -0.36882 (39)  | 0.16443 (30) | 2.34 (13)                  | 2.34 (13)                  | 2.30 (17)                  |
| D3 | 0.11725 (63)  | $-\frac{1}{4}$ | 0.41252 (54) | 2.17 (21)                  | 4.89 (24)                  | 3.62 (26)                  |
| D4 | -0.10108 (43) | -0.12664 (38)  | 0.41753 (35) | 3.96 (16)                  | 1.94 (13)                  | 3.14 (19)                  |

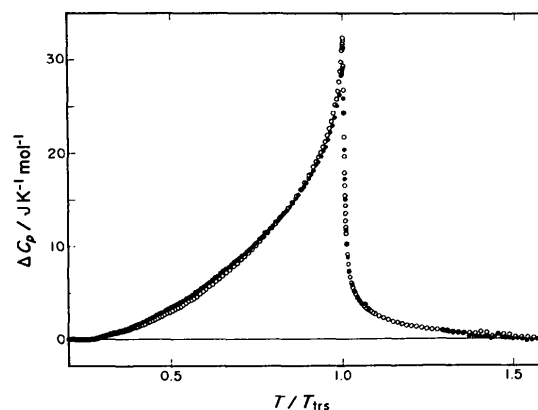
The temperature regions where the experimental heat capacities were used for the fitting were 13–40 and 250–303 K, as used in the comparable calculation for CH<sub>3</sub>NH<sub>3</sub>I. The fitted line reproduced the experimental data as shown in Fig. 8, where the contribution from each term is shown separately. The best-fit values of the parameters were as follows:  $\theta_D = 81.1$  K,  $\theta_E = 143.7$  K, and  $A = 1.56 \times 10^{-6}$  J<sup>-1</sup> mol.

Fig. 7. Molar heat capacities of CD<sub>3</sub>ND<sub>3</sub>I (○) and CH<sub>3</sub>NH<sub>3</sub>I (●).Fig. 8. The heat-capacity curve of CD<sub>3</sub>ND<sub>3</sub>I separated into the various contributions. (A) Intra-ionic vibration, (B) libration, (C) internal rotation, (D) overall rotation, (E) lattice vibration (Einstein), (F) lattice vibration (Debye), (G)  $C_p - C_v$  correction.

Both of the Debye and Einstein temperatures are lower than those of CH<sub>3</sub>NH<sub>3</sub>I ( $\theta_D = 83.6$  K and  $\theta_E = 171.2$  K), which reflects the mass effect on the vibrations.

The anomalous heat capacities derived by subtracting the base line from the total are shown as open circles in Fig. 9. Those of CH<sub>3</sub>NH<sub>3</sub>I are also shown for comparison as closed circles. The temperature scale is reduced by the respective transition temperatures (164.0 K for CD<sub>3</sub>ND<sub>3</sub>I and 166.1 K for CH<sub>3</sub>NH<sub>3</sub>I). Clearly, the anomalous heat capacity of CD<sub>3</sub>ND<sub>3</sub>I closely resembles that of CH<sub>3</sub>NH<sub>3</sub>I in the whole temperature region. The entropy of the transition of CD<sub>3</sub>ND<sub>3</sub><sup>+</sup> was 8.8 J K<sup>-1</sup> mol<sup>-1</sup>, which is also close to that of CH<sub>3</sub>NH<sub>3</sub>I (9.3 J K<sup>-1</sup> mol<sup>-1</sup>). As described above the C–N axis of the CD<sub>3</sub>ND<sub>3</sub><sup>+</sup> ion has a threefold axis located on the fourfold crystallographic axis. The transition entropy therefore should ideally be  $R \ln 4$  (= 11.5 J K<sup>-1</sup> mol<sup>-1</sup>) in the static limit. The smaller experimental value for the transition entropy is probably related to the quasi-free rotation of the  $\alpha'$  phase as discussed previously (Yamamuro, Oguni, Matsuo & Suga, 1986*a,b*) and is in agreement with the neutron diffraction results.

Values for the molar heat capacities of CD<sub>3</sub>ND<sub>3</sub>I have been deposited along with the standard thermodynamic functions for CD<sub>3</sub>ND<sub>3</sub>I which derived from

Fig. 9. The anomalous heat capacities due to the  $\delta$ - $\alpha'$  transitions of CD<sub>3</sub>ND<sub>3</sub>I (○) and CH<sub>3</sub>NH<sub>3</sub>I (●).

the heat-capacity data. The base line function obtained in §3.3 was used for the extrapolation of the heat capacity in the temperature region 0–13 K.

#### 4. Summary

The studies described in this paper illustrate the complementary nature of calorimetric measurements and high-resolution neutron powder-diffraction data for the detailed elucidation of phase transitions in such molecular compounds. The heat-capacity measurements indicate a continuous phase transition from the tetragonal ( $P4/nmm$ )  $\alpha$  phase to the  $\delta$  phase suggesting the structure to be a subgroup of the former phase. This does prove to be the case as a distortion to an orthorhombic structure ( $Pbma$ ) results. The current work has provided valuable information towards an understanding of the overall phase behaviour and it is intended the structural information be combined with studies of the molecular rotations from which a fuller account of the phase behaviour mechanisms may be ascertained. Preliminary work would suggest some scheme of weak hydrogen bonding of the  $NH_3^+$  groups as a prerequisite for any such model.

The financial support given by the British Council for the present collaboration is gratefully acknowledged.

#### References

- ALBERT, S. & RIPMEESTER, J. A. (1973). *J. Chem. Phys.* **58**, 541.  
 ASTON, J. G. & ZIEMER, C. W. (1946). *J. Am. Chem. Soc.* **68**, 1405.

- CABANA, A. & SANDORFY, C. (1962). *Spectrochim. Acta*, **18**, 843.  
 CASTALLUCCI, E. (1969). *J. Mol. Struct.* **23**, 4040.  
 DAVID, W. I. F., AKPORIAYE, D., IBBERTSON, R. M. & WILSON, C. C. (1988). Report RAL-88-103. Rutherford Appleton Laboratory, Chilton, Didcot, Oxon, England.  
 GABE, E. J. (1961). *Acta Cryst.* **14**, 1296.  
 HENDRICKS, S. B. (1928). *Z. Kristallogr.* **67**, 106.  
 HUGHES, E. W. & LIPSCOMB, W. N. (1946). *J. Am. Chem. Soc.* **68**, 1970–1975.  
 ISHIDA, H., IKEDA, R. & NAKAMURA, D. (1982a). *J. Phys. Chem.* **86**, 1003.  
 ISHIDA, H., IKEDA, R. & NAKAMURA, D. (1982b). *Phys. Status Solidi A*, **70**, K151.  
 ISHIDA, H., IKEDA, R. & NAKAMURA, D. (1986). *Bull. Chem. Soc. Jpn*, **59**, 915.  
 JUGIE, G. & SMITH, J. A. S. (1978). *J. Chem. Soc. Faraday Trans. 2*, **74**, 994.  
 KELLER, E. (1988). *SCHAKAL. A Fortran Program for the Graphical Representation of Molecular and Crystallographic Models*. Albert-Ludwigs-Univ., Freiburg, Germany.  
 LUDMAN, C. J., RATCLIFFE, C. I. & WADDINGTON, T. C. (1976). *J. Chem. Soc. Faraday Trans. 2*, **72**, 1759.  
 MATSUO, T. & SUGA, H. (1985). *Thermochim. Acta*, **88**, 149.  
 PAWLEY, G. S. (1981). *J. Appl. Cryst.* **14**, 357–361.  
 PAWLEY, G. S. & HEWAT, A. W. (1985). *Acta Cryst.* **B41**, 136–139.  
 STAMMLER, M. (1967). *J. Inorg. Nucl. Chem.* **29**, 2203.  
 SUNDARAM, C. S. & RAMAKRISHNA, J. (1982). *J. Curr. Sci.* **51**, 835.  
 TATSUMI, M., MATSUO, T., SUGA, H. & SEKI, S. (1975). *Bull. Chem. Soc. Jpn*, **48**, 3060.  
 TEGENFELDT, J., KEOWSIM, T. & SÄTERKVIST, C. S. (1972). *Acta Chem. Scand.* **26**, 3524.  
 THÉORËT, A. & SANDORFY, C. (1967). *Spectrochim. Acta*, **23A**, 519.  
 TSAU, J. & GILSON, D. F. R. (1970). *Can. J. Chem.* **48**, 717.  
 WERNER, P. E. (1976). *J. Appl. Cryst.* **9**, 216–219.  
 WHALLEY, E. (1969). *J. Chem. Phys.* **51**, 4040.  
 YAMAMURO, O., OGUNI, M., MATSUO, T. & SUGA, H. (1986a). *J. Chem. Thermodyn.* **18**, 939.  
 YAMAMURO, O., OGUNI, M., MATSUO, T. & SUGA, H. (1986b). *Thermochim. Acta*, **98**, 327.  
 YAMAMURO, O., OGUNI, M., MATSUO, T. & SUGA, H. (1987). *Bull. Chem. Soc. Jpn*, **60**, 779.